

MISSING RESONANCES IN KAON PHOTOPRODUCTION ON THE NUCLEON

T. MART, A. SULAKSONO

Departemen Fisika, FMIPA, Universitas Indonesia, Depok 16424, Indonesia

C. BENNHOLD

*Center for Nuclear Studies, Department of Physics, The George Washington
University, Washington, D.C. 20052, USA*

New kaon photoproduction data on a proton, $\gamma + p \rightarrow K^+ + \Lambda$, are analyzed using a multipole approach. The background terms are given in terms of gauge invariant, crossing symmetric, Born diagrams with hadronic form factors, while the resonances are parameterized using Breit-Wigner forms. Preliminary results suggest a number of new resonances, as predicted by many quark model studies. A comparison between the extracted multipoles and those obtained from KAON-MAID is presented.

1. Introduction

Considerable theoretical and experimental efforts to understand the structure of the nucleon have been devoted for more than fifty years. A consequence of this substructure is the nucleon resonance spectra found in the region between 1 - 3 GeV. This region is accessible neither through perturbative QCD at high energies nor through chiral perturbation theory at low energies. There is hope that lattice QCD will provide answers through numerical techniques. Meanwhile, our knowledge of resonance physics comes mostly from phenomenology. This paper presents a new investigation of the nucleon spectrum through the photoproduction of a kaon on a proton. To this end, we will make use of a multipole approach to describe the resonant states. Such studies have been reported by previous authors^{1,2}, albeit using a limited data base. We report preliminary results using the new data that have become available this year from SAPHIR³ and JLAB⁴.

2. Formalism

2.1. Background Amplitudes

The basic background amplitudes are obtained from a series of tree-level Feynman diagrams, shown in previous work^{1,5,6,12}. They contain the standard s , u , and t -channel Born terms along with the $K^*(892)$ and $K_1(1270)$ t -channel poles. Apart from the $K_1(1270)$ exchange, these background terms are similar to the ones used by Thom¹. The importance of the $K_1(1270)$ intermediate state has been pointed out in Ref.⁷. To account for the hadronic structures of interacting baryons and mesons we include the appropriate hadronic form factors in the hadronic vertices by utilizing Haberzettl's method¹⁰ in order to maintain gauge invariance of the amplitudes. Furthermore, to comply with the *crossing symmetry* requirement we use a special form factor in the *gauge terms*, as has been proposed by Davidson and Workman¹¹. Thus, compared to the previous pioneering work¹, the major advancement in the background sector is the use of hadronic form factors to control its contribution in a gauge-invariant and the crossing-symmetric fashion.

2.2. Resonance Amplitudes

The resonant electric and magnetic multipoles for a state with the mass M_R , width Γ , and angular momentum l are assumed to have the Breit-Wigner form

$$E_{l\pm}, M_{l\pm} = \left\{ \frac{1}{k_R q_R j_\gamma(j_\gamma + 1)} \frac{v_l(qR)}{v_l(q_R R)} \right\}^{1/2} \frac{M_R \Gamma \sqrt{\Gamma_{\gamma E(M)} \Gamma_K} e^{i\theta}}{M_R^2 - s - iM_R \Gamma}, \quad (1)$$

where s represents the square of the total c.m. energy, k_R and q_R are the photon and kaon momenta evaluated at the resonance's pole ($s = M_R^2$), θ is the phase angle, $j_\gamma = l \pm 1$ for $E_{l\pm}$ and $j_\gamma = l$ for $M_{l\pm}$. The factors $\Gamma_{\gamma E(M)}$ and Γ_K represent the branching ratios of the resonance into γp and $K^+ \Lambda$, respectively.

The $v_l(qR)$ denote Blatt-Weisskopf barrier penetration factors which accounts for the dependency of partial decay widths on the momentum and

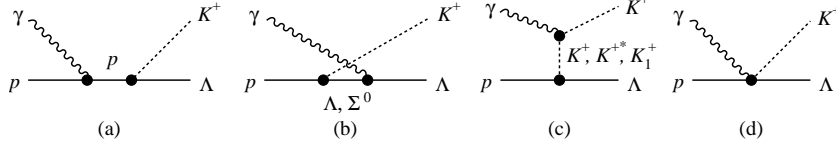


Figure 1. Contribution of the s -, u -, and t -channel to the background amplitudes for kaon photoproduction on the nucleon $\gamma + p \rightarrow K^+ + \Lambda$. The contact diagram (d) is required to restore gauge invariance after introducing hadronic form factors.

are given by¹⁵

$$\begin{aligned}
v_0(x) &= 1, \\
v_1(x) &= x^2/(1+x^2), \\
v_2(x) &= x^4/(9+3x^2+x^4), \\
v_3(x) &= x^6/(225+45x^2+6x^4+x^6), \\
v_4(x) &= x^8/(11025+1575x^2+135x^4+10x^6+x^8),
\end{aligned} \tag{2}$$

Following Thom¹, in this calculation the interaction radius R has been fixed at about one Fermi ($1/R = 200$ MeV). All observables can be calculated from the CGLN amplitudes¹⁶

$$F = i\boldsymbol{\sigma} \cdot \boldsymbol{\epsilon} F_1 + \boldsymbol{\sigma} \cdot \hat{\mathbf{q}} \boldsymbol{\sigma} \cdot (\hat{\mathbf{k}} \times \boldsymbol{\epsilon}) F_2 + i\boldsymbol{\sigma} \cdot \hat{\mathbf{k}} \hat{\mathbf{q}} \cdot \boldsymbol{\epsilon} F_3 + i\boldsymbol{\sigma} \cdot \hat{\mathbf{q}} \hat{\mathbf{q}} \cdot \boldsymbol{\epsilon} F_4, \tag{3}$$

where the amplitudes F_i are related to the electric and magnetic multipoles given in Eq. (1) for up to $l = 4$ by

$$\begin{aligned}
F_1 &= E_{0+} - \frac{3}{2}(E_{2+} + 2M_{2+}) + E_{2-} + 3M_{2-} \\
&\quad + \frac{15}{8}(E_{4+} + 4M_{4+}) - \frac{3}{2}(E_{4-} + 5M_{4-}) \\
&\quad + 3 \{ E_{1+} + M_{1+} - \frac{5}{2}(E_{3+} + 3M_{3+}) + E_{3-} + 4M_{3-} \} \cos \theta \\
&\quad + \frac{15}{2} \{ E_{2+} + 2M_{2+} - \frac{7}{2}(E_{4+} + 4M_{4+}) + E_{4-} + 5M_{4-} \} \cos^2 \theta \\
&\quad + \frac{35}{2}(E_{3+} + 3M_{3+}) \cos^3 \theta + \frac{315}{8}(E_{4+} + 4M_{4+}) \cos^4 \theta,
\end{aligned} \tag{4}$$

$$\begin{aligned}
F_2 &= 2M_{1+} + M_{1-} - \frac{3}{2}(4M_{3+} + 3M_{3-}) \\
&\quad + 3 \{ 3M_{2+} + 2M_{2-} - \frac{5}{2}(5M_{4+} + 4M_{4-}) \} \cos \theta \\
&\quad + \frac{15}{2}(4M_{3+} + 3M_{3-}) \cos^2 \theta + \frac{35}{2}(5M_{4+} + 4M_{4-}) \cos^3 \theta,
\end{aligned} \tag{5}$$

$$\begin{aligned}
F_3 &= 3 \{ E_{1+} - M_{1-} - \frac{5}{2}(E_{3+} - M_{3+}) + E_{3-} + M_{3-} \} \\
&\quad + 15 \{ E_{2+} - M_{2+} + E_{4-} + M_{4-} - \frac{7}{2}(E_{4+} - M_{4+}) \} \cos \theta \\
&\quad + \frac{105}{2}(E_{3+} - M_{3+}) \cos^2 \theta + \frac{315}{2}(E_{4+} - M_{4+}) \cos^3 \theta,
\end{aligned} \tag{6}$$

$$\begin{aligned}
F_4 = 3 \{ & M_{2+} - E_{2+} - M_{2-} - E_{2-} - \frac{5}{2}(M_{4+} - E_{4+} - M_{4-} - E_{4-}) \} \\
& + 15(M_{3+} - E_{3+} - M_{3-} - E_{3-}) \cos \theta + \frac{105}{2}(M_{4+} - E_{4+} \\
& - M_{4-} - E_{4-}) \cos^2 \theta .
\end{aligned} \tag{7}$$

These amplitudes are combined with the CGLN amplitudes obtained from the background terms^{1,12} and substituted into Eq. (3).

3. Results and Discussion

In Ref.² Tanabe *et al.* put forward a model which contains the resonances in the partial waves S_{11} , P_{11} , P_{13} , D_{13} , and G_{17} resonances to fit the old $K^+\Lambda$ photoproduction data. It is well known that the $K^+\Lambda$ threshold region is dominated by the states $S_{11}(1650)$, $P_{11}(1710)$, and $P_{13}(1720)$. For our analysis, we allow states up to spin 7/2 to contribute. Sample preliminary results are shown in Table 1, where we explored the sensitivity of the data to two separate resonant states at different energies in the same partial wave, as predicted in some quark models¹⁸. In the fitting procedure, we constrain the mass of all resonances to vary between 1600 and 2200 MeV. For certain partial waves, such as D_{15} and F_{17} , the fit generates spurious states in close proximity to each other (Model I). Yet, fits with only one state in each of these partial waves lead the states with masses quite different from what is found before (Model II), indicating that the results presented here cannot be yet be interpreted as signaling new resonances in these partial waves.

We summarize the results as follows:

- S_{11} states
In the two models the mass of the first S_{11} does not significantly change, this first S_{11} is clearly related to the four-star S_{11} in the PDG table. A second S_{11} state appears above 2 GeV but its position does not remain fixed.
- P_{11} states
The fit prefers two states in this partial wave, one at lower energy around 1700 MeV and one in the 1850-1900 MeV mass region. The width of the lower state turns out to be surprisingly narrow with 100 MeV, casting doubt on the interpretation that this state is the $P_{11}(1710)$ resonance that is usually found with a much broader width of 300 - 400 MeV.
- P_{13} states
This situation is similar to the P_{11} case. Two states are preferred by the fit, the lower with a mass below 1700 MeV, possibly cor-

Table 1. Resonance states and their parameters extracted from fit to models I and model II. The units for M , Γ , $\sqrt{\Gamma_\gamma \Gamma_K}$, and θ are given in MeV, MeV, 10^{-3} MeV, and deg., respectively.

Resonance	Model I				Model II				
	M	Γ	$\sqrt{\Gamma_\gamma \Gamma_K}$	θ	M	Γ	$\sqrt{\Gamma_\gamma \Gamma_K}$	θ	
S_{11} E_{0+}	1610	365	3.38	13.8	1610	354	4.12	13.5	
S_{11} E_{0+}	2043	283	7.76	-76.5	2200	400	-4.94	91.2	
P_{11} M_{1-}	1728	100	6.17	-180.0	1707	100	5.00	152.3	
P_{11} M_{1-}	1893	312	12.28	87.7	1836	100	1.92	-180.0	
P_{13} E_{1+}	1654	184	5.79	-42.6	1688	121	5.45	-8.26	
	M_{1+}	-	-	-3.29	-	-	-	-2.97	-
P_{13} E_{1+}	1909	240	-3.68	140.3	1850	400	3.67	-41.1	
	M_{1+}	-	-	-1.33	-	-	-	-2.61	-
D_{13} E_{2-}	2200	183	4.45	-94.2	1912	148	-5.72	156.7	
	M_{2-}	-	-	-1.11	-	-	1.64	-	
D_{13} E_{2-}	1741	315	1.50	90.4	1750	252	-0.62	-66.9	
	M_{2-}	-	-	4.49	-	-	-4.15	-	
D_{15} E_{2+}	1780	151	11.59	-21.4	2179	400	-4.07	179.9	
	M_{2+}	-	-	0.53	-	-	1.83	-	
D_{15} E_{2+}	1774	105	9.30	148.8	-	-	-	-	
	M_{2+}	-	-	3.05	-	-	-	-	
F_{17} E_{3+}	1921	343	-11.36	180.0	1715	100	-0.69	128.7	
	M_{3+}	-	-	-6.01	-	-	0.94	-	
F_{17} E_{3+}	1900	315	11.64	171.7	-	-	-	-	
	M_{3+}	-	-	5.69	-	-	-	-	
G_{17} E_{4-}	1723	100	0.05	116.6	1730	100	0.25	180.0	
	M_{4-}	-	-	0.41	-	-	0.14	-	
G_{17} E_{4-}	2082	133	0.52	-180.0	2011	400	1.59	-10.1	
	M_{4-}	-	-	-1.19	-	-	1.37	-	
$\chi^2/\text{d.o.f.}$	0.85				0.91				

responding to the $P_{13}(1720)$ and a state at higher energy with a broader width of 250 - 400 MeV.

- D_{13} states

Using quark model predictions as guidance, a previous analysis⁸ suggested that a new resonance in this partial wave, the $D_{13}(1900)$, provides an explanation for the new structure found in the old SAPHIR data around 1900 MeV. Our new results with the new data point a more confusing and still incomplete picture, the fits find a lower state around 1750 MeV, while the mass of the higher state appears to be ill determined.

- D_{15} and F_{17} states

In both partial waves, the fit clearly rejects two separate states,

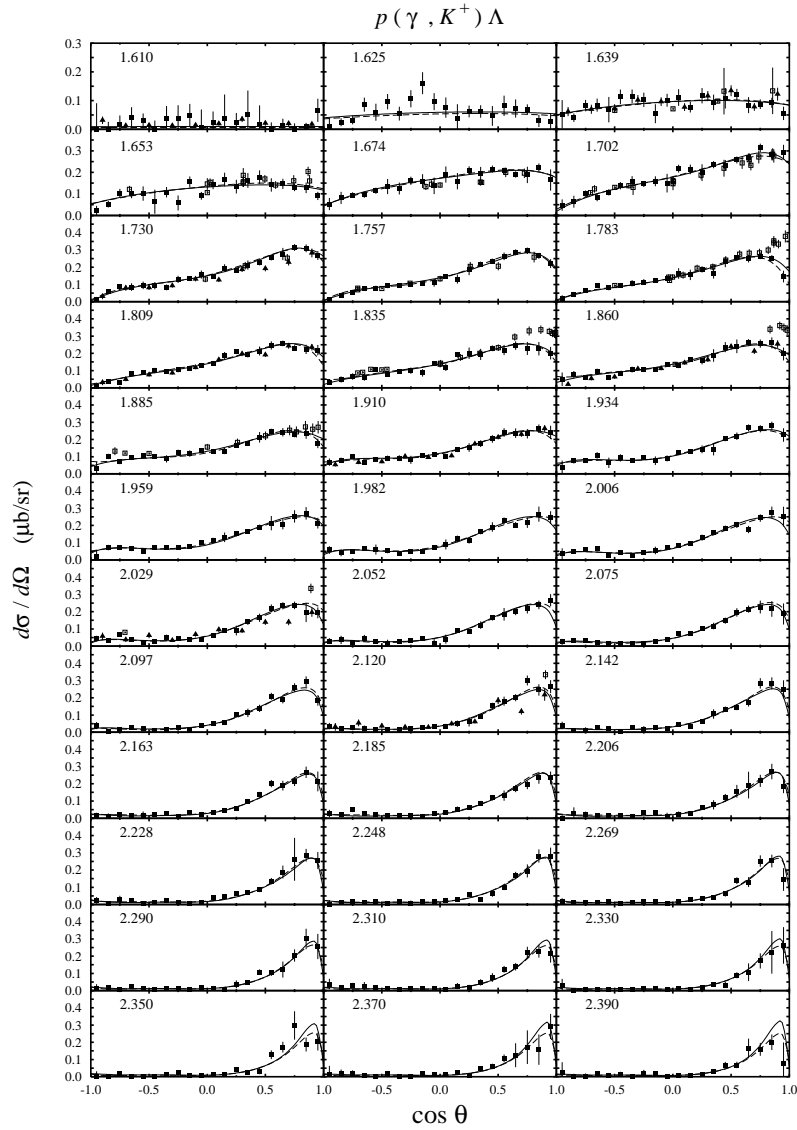
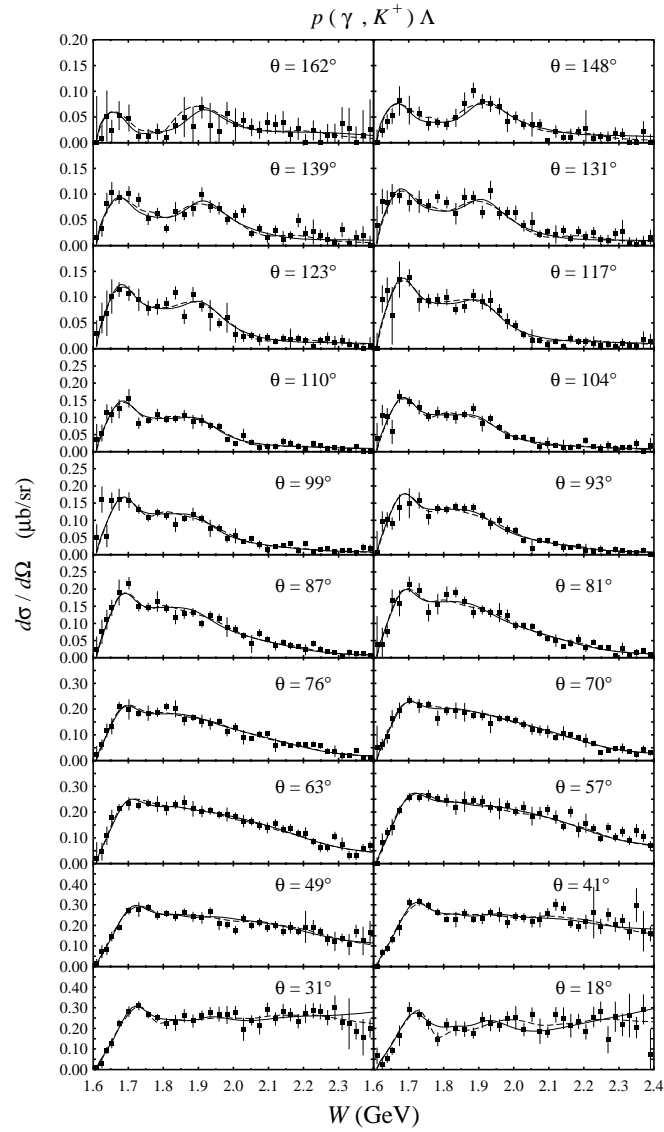


Figure 2. The $p(\gamma, K^+) \Lambda$ differential cross sections as a function of kaon angle. Dashed and solid lines refer to the Model I and II of Table 1, respectively. Data are taken from Ref. 3,13.

Figure 3. Same as in Fig. 2, but for W distribution.

yet when combined into one resonance, the mass turns out to be unstable. It is not clear yet if resonances are really needed in these partial waves or if these phenomena are mocking up missing

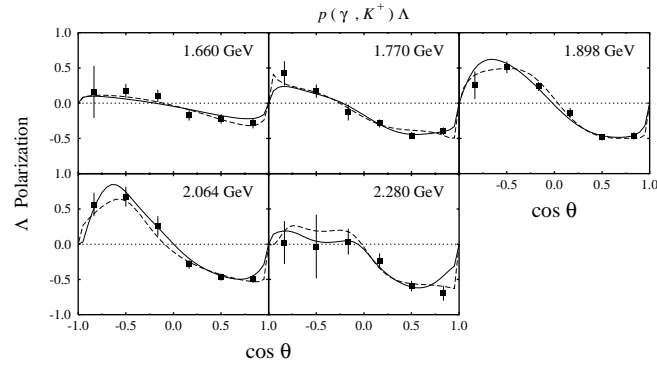


Figure 4. The Λ recoil polarization for the $p(\gamma, K^+)\Lambda$ reaction. Notations are as in Fig 2.

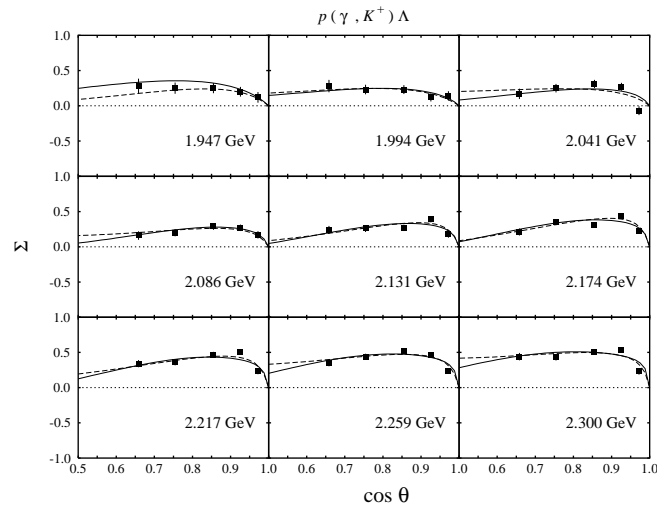


Figure 5. Photon asymmetry for the $p(\gamma, K^+)\Lambda$ reaction. Notations are as in Fig 2.

background physics.

- G_{17} states

The only well-known state in this partial wave is around 2100 MeV, a new state with a mass as low as 1750, as suggested by our fit, would be surprising. Further studies will have to verify if this state is in fact required to fit the data.

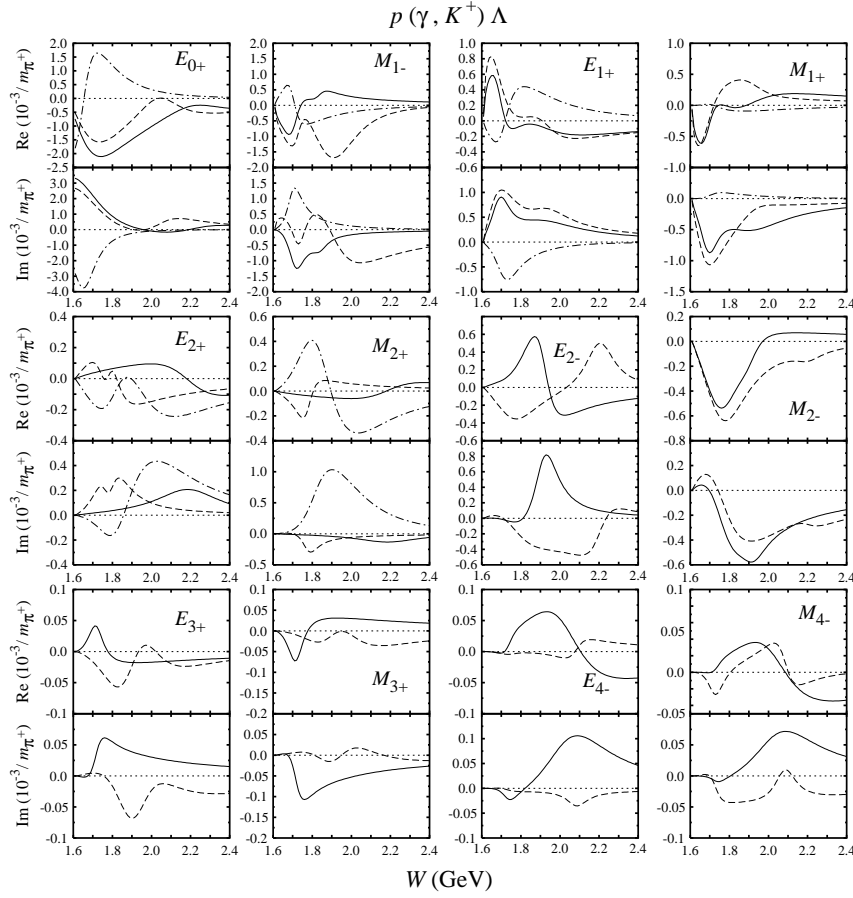


Figure 6. Electric and magnetic multipoles for the $p(\gamma, K^+)\Lambda$ reaction. Dashed and solid lines represent Model I and Model II of Table 1. Dash-dotted lines display the multipoles obtained from the KAON-MAID solution¹⁷, where only resonances with $l \leq 2$ are included.

These sample results display the difficulty in identifying a unique set of resonances required to fit the data. Clearly, minimization of the χ^2 cannot be the only criterion for establishing a new resonance but one must achieve consistency with other reactions through a genuine multichannel analysis.

Figures 2-5 compare the model fits with the available differential cross section and polarization data. As expected from the two χ^2 the models are virtually indistinguishable in these observables, yet can lead to very differ-

ent multipoles, as shown in Figure 6. Clearly, more polarization data are needed that should permit a more model-independent multipole analysis.

Acknowledgment

This work was supported in part by the QUE project (TM and AS) and the U.S. Department of Energy contract no. DE-FG02-95ER-40907 (CB).

References

1. H. Thom, *Phys. Rev.* **151**, 1322 (1966).
2. H. Tanabe, M. Kohno and C. Bennhold, *Phys. Rev.* **C39**, 741 (1989).
3. K. H. Glander *et al.*, *Eur. Phys. J. A* **19**, 251 (2004)
4. J. W. C. McNabb *et al.* [The CLAS Collaboration], *Phys. Rev. C* **69**, 042201 (2004)
5. F. X. Lee, T. Mart, C. Bennhold, H. Habertzettl and L. E. Wright, *Nucl. Phys.* **A695**, 237 (2001).
6. R. A. Adelseck and B. Saghai, *Phys. Rev.* **C42**, 108 (1990).
7. R. A. Adelseck and L. E. Wright, *Phys. Rev.* **C38**, 1965 (1988).
8. T. Mart and C. Bennhold, *Phys. Rev.* **C61**, 012201 (2000).
9. R. A. Arndt, I. I. Strakovsky, R. L. Workman and M. M. Pavan, *Phys. Rev.* **C52**, 2120 (1995).
10. H. Habertzettl, C. Bennhold, T. Mart and T. Feuster, *Phys. Rev.* **C58**, 40 (1998).
11. R. M. Davidson and R. Workman, *Phys. Rev.* **C63**, 025210 (2001).
12. J. C. David, C. Fayard, G. H. Lamot and B. Saghai, *Phys. Rev.* **C53**, 2613 (1996).
13. M. Q. Tran *et al.*, *Phys. Lett.* **B445**, 20 (1998).
14. K. Hagiwara *et al.*, *Phys. Rev.* **D66**, 010001 (2002).
15. J. M. Blatt and V. F. Weisskopf, *Theoretical Nuclear Physics* (John Wiley & Sons, New York, 1952).
16. G. Knochlein, D. Drechsel and L. Tiator, *Z. Phys.* **A352**, 327 (1995).
17. See: <http://www.kph.uni-mainz.de/MAID/kaon/kaonmaid.html>
18. S. Capstick and W. Roberts, *Phys. Rev. D* **58**, 074011 (1998).